2024 IEEE/RSJ International Conference on Intelligent Robots and Systems (IROS)
October 14-18, 2024. Abu Dhabi, UAE

Under-actuated Robotic Gripper with Multiple Grasping Modes Inspired by Human Finger

Jihao Li[1,2], Tingbo Liao[3], Hassen Nigatu[1,2], Haotian Guo[1,2], Guodong Lu[2], and Huixu Dong[1,2,*]

***Abstract*— Under-actuated robot grippers, as a pervasive tool of robots, have become a considerable research focus. Despite their simplicity of mechanical design and control strategy, they suffer from poor versatility and weak adaptability, making widespread applications limited. To better address relevant research gaps, we present a novel 3-finger linkage-based gripper that realizes retractable and reconfigurable multi-mode grasps driven by a single motor. Firstly, inspired by the changes occurred in the contact surface with a human finger moving, we artfully design a slider-slide rail mechanism as the phalanx to achieve retraction of each finger, allowing for better performance in the enveloping grasping mode. Secondly, a reconfigurable structure is constructed to broaden the grasping range of objects' dimensions for the proposed gripper. By adjusting the configuration and gesture of each finger, the gripper can achieve five grasping modes. Thirdly, the proposed gripper is solely actuated by a single motor, yet it can be capable of grasping and reconfiguring simultaneously. Finally, various experiments on grasps of slender, thin, and large-volume objects are implemented to evaluate the performance of the proposed gripper in practical scenarios, which demonstrates the excellent grasping capabilities of the gripper.**

I. INTRODUCTION

As grasping is a crucial capability of robots, numerous robot grippers have been developed as grasping executive tools to be applied in various fields, such as logistics, warehousing scenarios, industrial settings, and human-computer interaction [1]–[3]. Among various grippers, the full-actuated grippers have improved dexterity, owing to the independent motion of each joint [4]. However, it brings about issues in the high cost and complexity of the mechanism and control. Therefore, under-actuated grippers have attracted substantial attention, which is advantageous in simplifying the mechanical design, control strategy and improving the grasping adaptability as well as reducing the cost [5].

Prevalent under-actuated grippers can be broadly categorized into soft and rigid types [6], [7]. The soft grippers are typically constructed via lightweight and flexible materials, driven by tendons or pneumatic/hydraulic systems [8]–[10]. They prioritize safety, versatility, and adaptability in robotic manipulation, offering a stable grasp of objects with complex contours. For instance, Gunderman *et al.* [8] presented a tendon-driven soft robotic gripper with passive compliance, while Wang *et al.* [9] presented a pneumatic-driven gripper that is able to vary its stiffness and working length. Nevertheless, they have a low load capacity and a short lifespan due to material properties. In contrast, the structure of rigid grippers is dominated by linkage and gear systems, which are known for their stiffness and precision [11], [12]. Toshihiro *et al.* [13] utilized chuck clamping devices to create a gripper. A gripper with fingers that are scissor linkages was proposed by Kwon *et al.* [11]. However, these grippers cannot adjust the grasping range and adapt to objects with irregular shapes, resulting in unstable grasping. To alleviate these drawbacks, certain grippers were designed by mimicking the human finger to flex and relax muscles for modifying contact surface areas [14]. This feature significantly improves the graspable range and dexterity of the human hand, allowing it to grasp even slender or thin objects with a single finger. Notably, Bandara *et al.* [15] built an under-actuated gripper based on a modified cross-bar mechanism. Abayasiri *et al.* [16] proposed a humanoid robotic hand that employs a 5-linkage mechanism. Yet, these rigid grippers, which are designed to imitate the motion of human fingers, cannot achieve changes in contact surface caused by muscle contraction, which limits their adaptability and envelopment capabilities. To enhance the flexibility of robot grippers, some grippers are designed with reconfiguration mechanisms [17], [18]. However, these grippers rely on additional motors to rotate or translate the

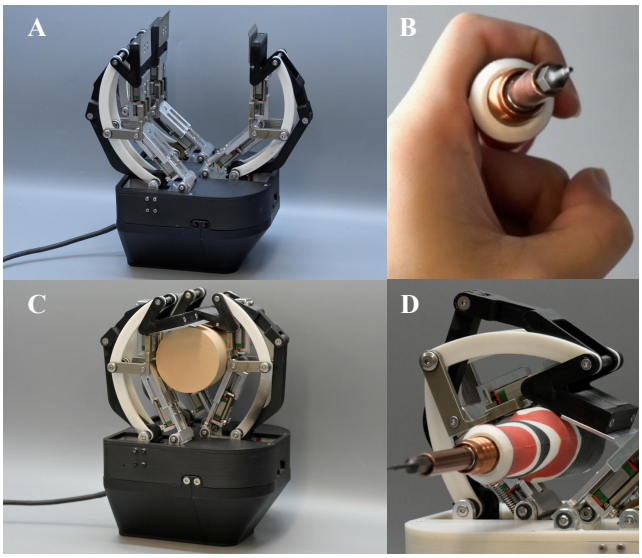

Figure. 1. The prototype of presented gripper (A, C), grasp slender and thin objects through the human finger (B) and the presented gripper (D).

This work was supported by National Natural Science Foundation of China (Youth Program:509109-N72401), Natural Science Foundation of Zhejiang Province (509109-N82401) and State Key Laboratory of Fluid Power & Mechatronic System (509116*A62403/103).

[1]Grasp Lab, School of Mechanical Engineering, Zhejiang University, Hangzhou 310027, China.
[2]Robotics Institute of Zhejiang University, Hangzhou 310027, China.
[3]College of Design and Engineering National University of Singapore, 117575, Singapore.
Email: {huixudong, lijihao}@zju.edu.cn
*Corresponding author

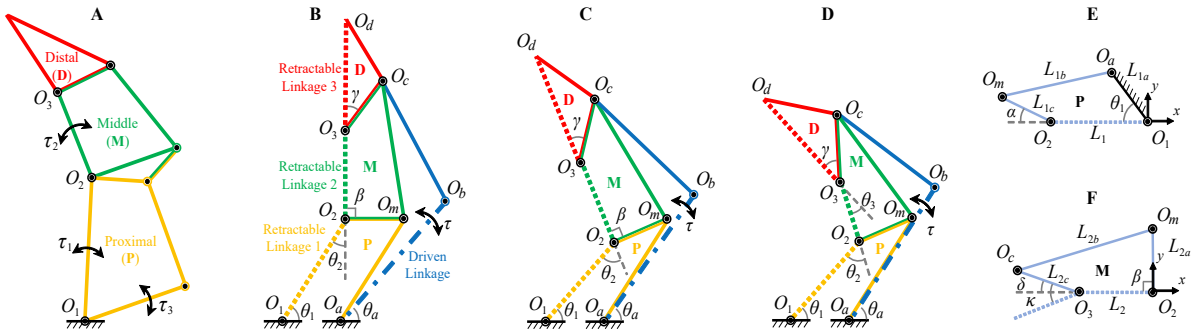

Figure. 2. A general three-phalanx finger comprise the metacarpophalangeal (MCP) joint, proximal interphalangeal (PIP) joint and distal interphalangeal (DIP) joint (A). The prototype of the proposed gripper: the parallel grasp mode (B), and the enveloping grasp mode (C/D). The thick dotted line represents the driven linkage, and the dotted line indicates that the linkage is retractable. Kinematics model of the middle phalanx (E) and proximal phalanx (F).

fingers, resulting in a complex mechatronic system, such as the GTac gripper [17] and the SMS gripper [18]. Therefore, one current challenge is to develop a reconfigurable gripper that has the capability of grasping objects with a wide range of object dimensions and high adaptability.

To address the aforementioned issues, we propose a novel under-actuated gripper with three compressible fingers, as shown in Fig. 1. Firstly, the proximal phalanx is composed of a parallel four-bar linkage mechanism to achieve parallel grasping. In particular, each phalanx can achieve adaptive retraction through the designed slider-slide rail mechanism to perform enveloping grasping mode, ensuring stable grasping of objects of various volumes and shapes. Secondly, to minimize the number of gripper motors, a transmission mechanism including a worm, gears, and racks is artfully designed to distribute the output of the motor. In addition, a slotted block positioned proximal to the finger base is incorporated to constrain the movement of the finger during reconfiguration. Thus, the proposed gripper can achieve both grasping and reconfiguration abilities simultaneously through a single motor. Finally, the presented gripper can actively adjust the grasping range and passively switch between parallel grasping and enveloping grasping according to the shape of the objects, enabling the gripper to achieve up to five distinct grasping modes. As empirically validated through experimentation, the gripper exhibits notable traits, including elevated rigidity, substantial load-bearing capacity, robust adaptability, and a broad grasping range, which amalgamates the advantageous features of both rigid and soft grippers.

We **highlight** the **novelties** of our work. Foremost, our core contribution to this work is constructing a novel under-actuated gripper with capabilities of high adaptability and a large grasping range of object dimensions. The **first** novelty is that this work presents an innovative linkage mechanism to achieve the retraction of the phalanges for changing contact areas between the fingers and the objects, thereby varying the friction to improve the grasping stability. Although the proposed gripper is actuated by a single motor, it can perform grasping and reconfiguring simultaneously, considerably reducing the control and mechanism complexities, which is attributed to the **second** novelty. The **third** novelty is the capability to achieve five grasping modes by combining finger adaptability and reconfiguration. Different grasping modes can be employed to grasp objects with various sizes and contours, enhancing the stability of the grasp.

II. METHODOLOGY

A. Kinematic Analysis of the Under-actuated Finger

Three-joint fingers typically have 3 DOF and consist of the MCP joint, PIP joint, and distal DIP joint, as depicted in Fig. 2(A). The proposed gripper utilizes the retractable linkages L_1, L_2 and L_3 to constrain the motion of joints to achieve the purpose of under-actuation, as shown in Fig. 2(B) to (D).

Without external contact, retractable linkages L_1 and L_2 remain at their original lengths. In this state, the proximal phalanx ($O_1O_2O_mO_a$) is maintained in a flexible parallelogram mechanism by L_1, while the middle and distal phalanges combine to form a fixed five-bar mechanism ($O_2O_3O_dO_cO_m$). Since β is a fixed right angle, the orientation of the middle and distal phalanges will remain perpendicular to O_2O_m as the finger moves. This ensures the parallel grasping mode of the gripper (see Fig. 2(B)) .

The angle of θ_1 is fixed and the gripper switches to enveloping grasp mode whenever the proximal phalanx contacts the object, as demonstrated in Fig. 2(C). The movement of the driven linkage compresses L_1, altering the shape of the proximal phalanx and changing the orientation of the middle phalanx. Yet, the middle and distal phalanges remain coupled due to the constraint of L_2. Similarly, when the middle phalanx comes into contact with the object, the angle of θ_2 is fixed, while L_2 is compressed. The distal phalanx and middle phalanges will be decoupled. Thus, the distal phalanx can move independently, allowing the finger to bend further to grasp thinner objects, as indicated in Fig. 2(D).

We construct the mathematical relationship between the angle of each joint and the length of each phalanx. Taking the proximal phalanx shown in Fig. 2(F) as an example, we analyze the length of retractable linkage L_1 after the finger moves. The vector-loop equation is provided as

$$\overrightarrow{O_1O_a} + \overrightarrow{O_aO_m} + \overrightarrow{O_mO_2} = \overrightarrow{O_1O_2} \tag{1}$$

The phalanx is composed of a four-bar linkage. Except for the retractable linkage L_1, the lengths of other linkages (L_{1a}, L_{1b}, L_{1c}) are constant. The angle α can be calculated based on the rotation angle of the finger,

$$\alpha = \beta - \theta_2 \tag{2}$$

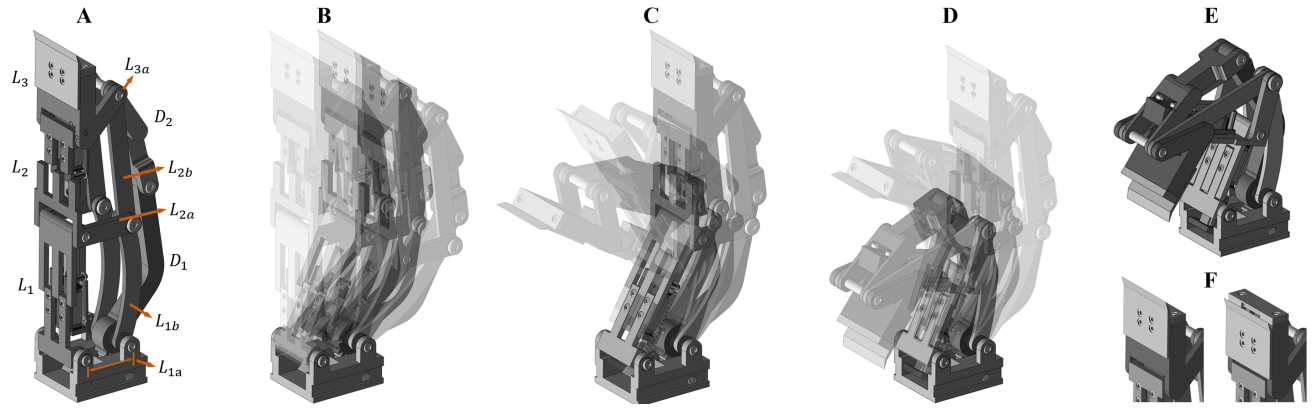

Figure. 3. Initial state (A); Parallel grasp (B) and Enveloping grasp (C, D); Maximum flexion state (E); The retractable ability of the distal phalanx (F).

A coordinate system is established at O_1, with $\overrightarrow{O_2O_1}$ representing the positive direction of the x-axis. Thus, the coordinates of O_2, O_m, and O_a can be obtained sequentially.

$$O_2(o_{2x}, o_{2y}) = (-L_1, 0) \tag{3}$$

$$O_m(o_{mx}, o_{my}) = (-L_1 - L_{1c}\cos(\alpha), L_{1c}\sin(\alpha)) \tag{4}$$

$$O_a(o_{ax}, o_{ay}) = (-L_{1a}\cos(\theta_1), L_{1a}\sin(\theta_1)) \tag{5}$$

To determine L_1, we substitute Eq. (3)-(5) into Eq. (1)

$$\begin{aligned} L_{1b}^2 = &(L_1 + L_{1c}\cos(\alpha) - L_{1a}\cos(\theta_1))^2 \\ &+ (L_{1a}\sin(\theta_1) - L_{1c}\sin(\alpha))^2 \end{aligned} \tag{6}$$

After algebraic manipulation, the quadratic polynomial representing L_1 can be derived

$$\begin{aligned} L_1^2 + b_1 L_1 + c_1 &= 0 \\ b_1 &= 2L_{1c}\cos(\alpha) - 2L_{1a}\cos(\theta_1) \\ c_1 &= L_{1a}^2 + L_{1b}^2 + L_{1c}^2 - 2L_{1a}L_{1c}\cos(\alpha - \theta_1) \end{aligned} \tag{7}$$

Therefore, the retractable linkage L_1 can be calculated by

$$L_1 = -\frac{1}{2}(b_1 \pm \sqrt{b_1^2 - 4c_1}) \tag{8}$$

In Fig. 3(B), the linkage L_{2a}, L_{2b}, L_{2c} and angle κ are constant. Similarly, the length of L_2 can be calculated by

$$\begin{aligned} \delta &= \kappa - \theta_3 \\ b_2 &= 2L_{2c}\cos(\delta) - 2L_{2a}\cos(\beta) \\ c_2 &= L_{2a}^2 + L_{2b}^2 + L_{2c}^2 - 2L_{2a}L_{2c}\cos(\delta - \beta) \\ L_2 &= -\frac{1}{2}(b_2 \pm \sqrt{b_2^2 - 4c_2}) \end{aligned} \tag{9}$$

The solutions with negative signs are used for determining the lengths of L_1 and L_2.

B. Design of the Under-actuated Finger

As previously stated, the inside linkage of each phalanx is the retractable linkage. As shown in Fig. 4(A), each retractable linkage comprises two sections: one section is connected to the MGN7C slider (17×22.5×6.5 mm) and the other section is connected to the MGN7 slide rail (7×4.8 mm). The two parts are constrained by the tension springs. The springs remain unstretched when there is no external force, and the retractable linkage retains its original length. When the phalanx is under stress, the tension springs gradually

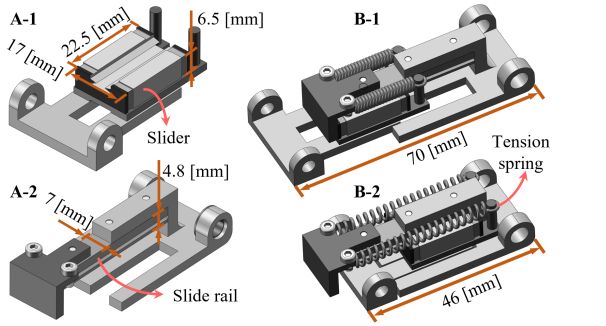

Figure. 4. Part connected to the slider (A-1). Part connected to the slide rail (A-2). Retractable linkage at its original length (B-1). Retractable linkage after being compressed (B-2).

stretch as the retractable linkage compresses. This procedure is illustrated in Fig. 4(B). To ensure smooth movement of the slider, the springs are installed symmetrically on both sides of the slide rail so that the resultant force is always along the direction of the slide rail and the resultant moment is 0. The types and parameters of the springs at each phalanx are:

- MCP joint : tension spring, K_{MCP} = 1 N/mm
- PIP joint : tension spring, K_{PIP} = 0.8 N/mm.
- DIP joint : compression spring, K_{DIP} = 0.55 N/mm.

The linkage length parameters for this finger are shown in Table I. Table II illustrates the theoretical parameters for the three retractable linkages after compression. Except for changes in linkage length, the flexion and mutual occlusion of the linkages will further affect the length of the finger contact surface. The actual contact surface length parameters of the phalanges are shown in Table III. Results show that the maximum compressibility of the phalanges is 57 mm. The actual contact length can be reduced by 74 mm. The minimum contact length is 57.95% of the original length.

During the actual grasping process, in the absence of external contact, the finger keeps in parallel grasp mode, as shown in Fig. 3(B). In Fig. 3(C), once the finger contacts the object, the proximal phalanx will retract first. As demonstrated in Fig. 3(D), once the middle phalanx contacts the object, it will start to retract, resulting in the decoupling of the middle and distal phalanges. Moreover, the distal phalanx also has a retractable function (see Fig. 3(F)), which is serving mainly for grasping thin objects and not participating in enveloping grasp. When grasping thin objects, this retractable linkage ensures that the fingertip is always in close contact with the

object placement surface, making it easier to pick up thin objects from the placement surface.

TABLE I

LINKAGE PARAMETER

Linkage	Length/mm	Linkage	Length/mm
D_1	85	L_2	55
D_2	68	L_{2a}	30
L_1	70	L_{2b}	76
L_{1a}	70	L_3	51
L_{1b}	30	L_{3a}	29

TABLE II

ANALYSIS OF LINKAGE LENGTH

Linkage	L_o/mm	L_c/mm	ΔL/mm	R_{theory}
L_1	70	46	24	34.29%
L_2	55	36	18	32.73%
L_3	51	36	15	29.41%
Total	176	119	57	32.39%

L_o, L_c, ΔL represent the original length, the shortest length after compression, and the change in length of each linkage, respectively. R_{theory} represents the theory ratio of the change in length.

TABLE III

ANALYSIS OF CONTACT LENGTH

Phalanx	S_o/mm	S_c/mm	ΔS/mm	$R_{practice}$
Proximal	70	40	30	42.86%
Middle	55	26	29	52.73%
Distal	51	36	15	29.41%
Total	176	102	74	42.05%

S_o, S_c, ΔS represent the original contact length, the shortest contact length after compression, and the change in contact length of each phalanx. $R_{practice}$ represents the practice ratio of the change in contact length.

C. Design of the Reconfiguration Mechanism

The proposed gripper has three fingers arranged crosswise on both sides, allowing the gripper to perform grasping and reconfiguration simultaneously with a single motor. The detail of the reconfiguration mechanism is described below:

To drive the fingers on both sides to perform correct motions, a gear set is introduced to allocate the power, as shown in Fig. 5. The gear set consists of a set of worm gears with a reduction ratio of 15:1 and several gears with 15 teeth in 1 mold (represented by g) and 30 teeth in 1 mold (represented by G). Notably, G_1 and G_3 are fixed to the shaft, while G_2 is only concentric with the shaft. Therefore, the magnitudes of the angular velocities of the three gears are equal, but the rotation direction of G_2 is opposite. The motor connected to the worm, and the Gear g_4 is connected to the worm gear, allowing the motor torque to be increased. The final motion of each gear is depicted in the figure.

Slide rails are installed on the bases of the gripper fingers. After assembly on the slide blocks, the entire translational motion of the fingers can be realized. Each transmission system consists of rack R (tooth down) and rack r (tooth up), which are installed in line and mesh with G and g_F, respectively (see Fig. 6(B)). G represents the three gears (G_1, G_2, G_3) at the final output of the gear set, and g_F represents the gear installed in each finger base. The rotation of the motor first drives G to translate the rack set. Then, the rack set drives g_F to rotate. Finally, g_F actuates the D_1 (the

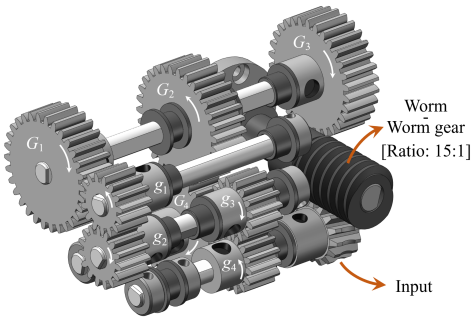

Figure. 5. 3D model of gear set.

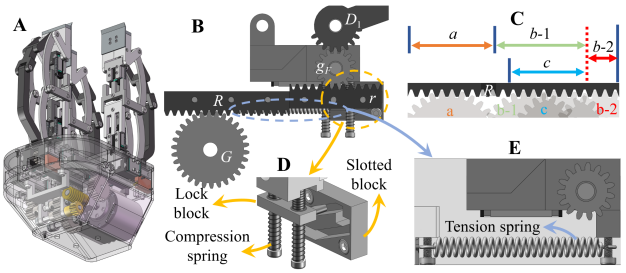

Figure. 6. 3D model of the gripper (A), Cross-sectional view of the rack group (B), each part of the rack corresponds to a specific controlled gripping mode (C), self-locking mechanism of reconfiguration components(D) and tension spring of reconfiguration components (E).

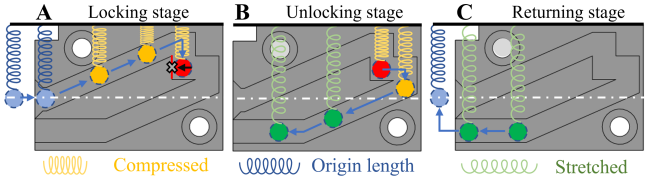

Figure. 7. Self-locking flow chart of self-locking mechanism.

driven linkage of each finger), enabling the fingers to move. In addition, a tension spring is installed between the finger base and the palm to constrain the reconfiguration of the fingers (see Fig. 6(E)). The overall prototype of the proposed gripper is shown in Fig. 6(A). Taking the direction of view in Fig. 6(B) as an example to analyze the opening and closing motion of the gripper:

When gear G rotates clockwise, it drives the rack R and r to translate to the right. Due to the constraint of the tension spring, the finger base initially remains stationary. Thus, r will drive g_F to rotate counterclockwise and linkage D_1 to rotate clockwise, ultimately realizing the opening of the gripper. Similarly, the counterclockwise motion of G will close the gripper. However, when the gripper is fully open, the clockwise rotation of linkage D_1 is limited. At this point, r will overcome the constraints of the tension spring and drive the entire finger base to move to the right, achieving reconfigurability. It should be noted that after the finger base moves to the far-right end, further counterclockwise motion of g_F will: 1) move the finger base to the left due to the tension of the spring, 2) actuate the finger that performs the closing motion. To achieve the closing action at the far-right end, a self-locking mechanism is introduced which limits the reverse movement of the finger base, as shown in Fig. 6(D). This mechanism consists of a lock block, a slotted block, and several compression springs. The top and bottom of the lock block are connected to the compression springs. The

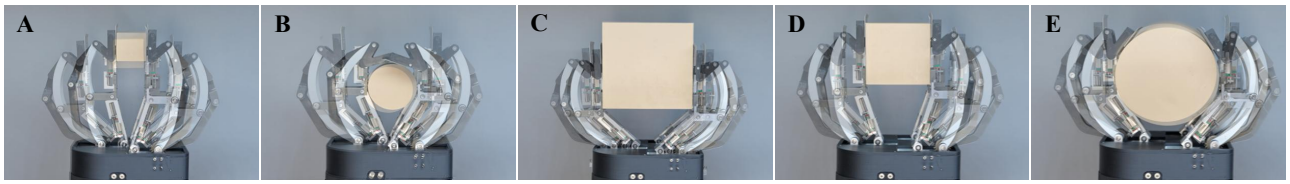

Figure. 8. Grasping procedure of each grasp mode: proximal parallel grasp mode(A), proximal enveloping grasp mode(B), translational grasp mode(C), remote parallel grasp mode(D) and remote enveloping grasp mode(E).

self-locking process is as follows (see Fig. 7).

• Locking stage (Fig. 7(A)): The lock block is in an equilibrium position before entering the slotted block. After entering the slotted block, it moves upward along the upper groove, compressing the spring accordingly. When the lock block crosses the incline, the spring pushes it down to the red position. If it moves in the opposite direction at this time, it will be restricted by the slotted block and cannot return. Correspondingly, if the finger base stops here, even if G rotates counterclockwise, the finger base will not be able to move to the left due to the self-locking mechanism. Therefore, r will give priority to driving linkage D_1, realizing the closing motion of the finger at the reconfigured position.

• Unlocking stage (Fig. 7(B)): When the lock block is at the red position, continue moving to the right, the lock block will enter the groove below. If the movement is reversed at this moment, the lock block moves along the groove below and is no longer constrained by the slotted block.

• Returning stage (Fig. 7(C)): When the lock block escapes the slotted block, it returns to the equilibrium position as the springs recover. Rotating G counterclockwise will return the finger to its original position.

The circle represents the part of the lock block that extends into the slotted block. The arrow indicates the movement direction of the lock block. The white, thin, dotted line is the equilibrium position of the lock block. This figure shows the state of the spring on the upper side of the lock block.

D. Description of Multi-grasping Mode

According to the grasping modes of the finger described above, combined with the reconfiguration function of the finger base, the proposed gripper can achieve a total of five grasping modes. As the gripper is actuated by a single motor, the control strategy is relatively straightforward and does not require an additional motor. Each grasping mode and its corresponding control strategy are described as follows:

- Mode 1 (proximal parallel grasp mode)
- Mode 2 (proximal enveloping grasp mode)
- Mode 3 (translational grasp mode)
- Mode 4 (remote parallel grasp mode)
- Mode 5 (remote enveloping grasp mode)

When G meshes with part a of the rack in Fig. 6(C), the gripper is in proximal grasping mode. The forward rotation of the motor will control the gripper to open, while the reverse rotation will close it. Notably, the adaptability of the fingers enables the gripper to autonomously switch between Mode 1 and Mode 2 based on the shape of the object. When the gear meshes with part b-1 of the rack, the motor's forward rotation will achieve Mode 3. As soon as gear G meshes with the red dotted line, the self-locking mechanism completes the locking and the gripper completes the reconfiguration. On the one hand, the self-locking mechanism unlocks when the motor rotation is reversed, coinciding with gear G meshing with the far-right end of part b-2. The finger will return to its original state from reconfiguration. On the other hand, if the motor is reversed immediately after the gear meshes with the red dotted line, the self-locking mechanism will stay locking. Following this, the gear shifts to mesh with part c of the rack, prompting the gripper to change to a mode suitable for remote grasping. By keeping the gear meshed with rack part c, the gripper automatically alternates between Mode 4 and Mode 5 for grasping, depending on the object's shape.

III. EXPERIMENTS

To evaluate the grasping performance of the proposed gripper, a prototype three-finger gripper was developed, and a series of experiments were conducted to verify the design: First, the implementation of five grasp modes was verified. Second, we verified the adaptability of the fingers and the reconfiguration function of the gripper by grasping standard objects and daily necessities.

A. Grasps at Different Grasping Modes

In the first experiment, the gripper was used to grasp a variety of objects with five distinct grasping modes, as depicted in Fig. 8. During the actual grasping process, it was observed that in the enveloping grasping modes (Mode 1 & Mode 4), all three joints were involved in grasping objects, resulting in a more stable grasp of the object. Whereas, in the parallel grasping modes (Mode 2 & Mode 3 & Mode 5), mainly DIP joints and PIP joints are engaged in grasping objects, leading to precise grasping performance, particularly in the translational grasping mode where the fingertips do not change height in the vertical direction, which enables fixed-point grasping of objects. From another perspective, the switching between parallel grasping mode and enveloping grasping mode (switching between Mode 1 & Mode 2 and switching between Mode 4 & Mode 5) is achieved through the retraction of phalanges, which passively adapts the MCP and DIP joints to the contour of the object. In contrast, the reconfiguration mechanism can actively adjust the grasping range by transitioning between the proximal grasping mode, translational grasping mode, and remote grasping mode.

B. Grasp Objects with Regular Shapes and Daily Necessities

The proposed gripper was mounted on the 6DOF industrial manipulator-UR3, and a series of grasping experiments were conducted to verify the performance of the gripper. To evaluate the versatility of the proposed gripper, we applied it

to grasp various objects. Fig. 9 depicts the cases of grasping regular objects with standard shapes, regular planes, regular arc surfaces, and irregular contours, respectively. Fig. 10(A) illustrates the use of a single finger to achieve grasping. In this state, the gripper is capable of gripping a 25 mm diameter cylinder. These grasping experiments prove that the gripper has a large grasping range and can adaptively adjust the finger posture according to the shape of the object.

However, the trajectory of the fingertip in the parallel grasping or enveloping grasping mode is arcuate. When grasping an object, the relative height between the fingertip and the object placement surface will change, which can make it hard for the gripper to grasp thin objects, especially since the gesture and position of the gripper are critically required. However, with the retractable function of the phalanx, thin objects can be grasped with ease. As the gripper closes and the fingertips contact the object placement surface, the distal phalanx and middle phalanx adaptively contract to ensure a smooth grasp. During the grasping process, the fingers are kept close to the surface on which the object is placed, allowing the gripper to better pick up thin objects. The specific grasping process is shown in Fig. 10. In Fig. 10(B), the fingertips begin to contact the object placement surface. In Fig. 10(C), the gripper adapts to the object placement surface during the closing process, and finally realizes the picking of thin objects (Fig. 10(D) and (E)).

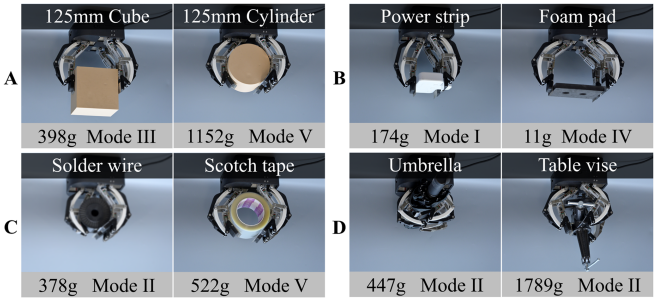

Figure. 9. Grasping objects with standard shapes(A); Grasping objects with regular plane (B); Grasping objects with regular arc surface (C); Grasping objects with irregular contour (D).

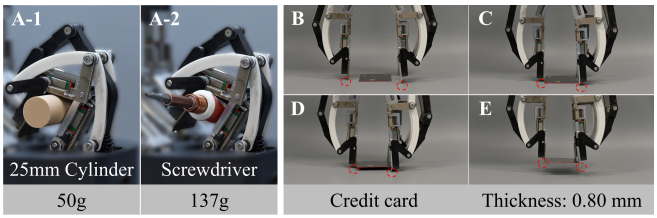

Figure. 10. The gripper utilizes the retractable function of its phalanges to grasp slender objects with one finger (A). Grasping is achieved with a single finger through the retractable function of the distal phalanx (B-E).

IV. CONCLUSIONS

In conclusion, this paper investigated a three-finger underactuated gripper featuring a retractable phalanx based on the linkage system. The proposed gripper not only achieved an extensive grasping range through its reconfiguration ability but also facilitated the automatic switching of grasping modes via finger retraction. Moreover, the implementation of a minimal number of motors objectively mitigated the challenges associated with gripper control. We conducted various grasping experiments to evaluate the real-world performance of the proposed gripper in diverse scenarios. The experimental results demonstrated impressive capabilities in terms of grasping stiffness, versatility, and adaptability.

REFERENCES

[1] H. Dong, Y. Feng, C. Qiu, and I.-M. Chen, "Construction of interaction parallel manipulator: towards rehabilitation massage," *IEEE/ASME Transactions on Mechatronics*, vol. 28, no. 1, pp. 372–384, 2022.

[2] H. Dong, E. Asadi, G. Sun, D. K. Prasad, and I.-M. Chen, "Real-time robotic manipulation of cylindrical objects in dynamic scenarios through elliptic shape primitives," *IEEE Transactions on Robotics*, vol. 35, no. 1, pp. 95–113, 2018.

[3] H. Dong, E. Asadi, C. Qiu, J. Dai, and I.-M. Chen, "Geometric design optimization of an under-actuated tendon-driven robotic gripper," *Robotics and Computer-Integrated Manufacturing*, vol. 50, pp. 80–89, 2018.

[4] J. Zhou, J. Yi, X. Chen, Z. Liu, and Z. Wang, "Bcl-13: A 13-dof soft robotic hand for dexterous grasping and in-hand manipulation," *IEEE Robotics and Automation Letters*, vol. 3, no. 4, pp. 3379–3386, 2018.

[5] L. Birglen, T. Laliberté, and C. M. Gosselin, *Underactuated robotic hands*, vol. 40. Springer, 2007.

[6] Z. Samadikhoshkho, K. Zareinia, and F. Janabi-Sharifi, "A brief review on robotic grippers classifications," in *2019 IEEE Canadian Conference of Electrical and Computer Engineering (CCECE)*, pp. 1–4, IEEE, 2019.

[7] H. Dong, C.-Y. Chen, C. Qiu, C.-H. Yeow, and H. Yu, "Gsg: A granary-shaped soft gripper with mechanical sensing via snap-through structure," *IEEE Robotics and Automation Letters*, vol. 7, no. 4, pp. 9421–9428, 2022.

[8] A. L. Gunderman, J. A. Collins, A. L. Myers, R. T. Threlfall, and Y. Chen, "Tendon-driven soft robotic gripper for blackberry harvesting," *IEEE Robotics and Automation Letters*, vol. 7, no. 2, pp. 2652–2659, 2022.

[9] Z. Wang and S. Hirai, "A soft gripper with adjustable stiffness and variable working length for handling food material," in *2018 IEEE International Conference on Real-time Computing and Robotics (RCAR)*, pp. 25–29, IEEE, 2018.

[10] Y. Li, Y. Chen, Y. Yang, and Y. Li, "Soft robotic grippers based on particle transmission," *IEEE/ASME Transactions on Mechatronics*, vol. 24, no. 3, pp. 969–978, 2019.

[11] J. Kwon, D. Bombara, C. Teeple, J. Lee, C. Hoberman, R. Wood, and J. Werfel, "Transformable linkage-based gripper for multi-mode grasping and manipulation," *IEEE Robotics and Automation Letters*, vol. 8, no. 12, pp. 8446–8453, 2023.

[12] G. A. Zappatore, G. Reina, A. Messina, *et al.*, "Analysis of a highly underactuated robotic hand," *Int. J. Mech. Control*, vol. 18, no. 2, pp. 17–24, 2017.

[13] T. Nishimura and T. Watanabe, "Single-motor robotic gripper with three functional modes for grasping in confined spaces," *IEEE Robotics and Automation Letters*, 2023.

[14] S. J. Yoon, M. Choi, B. Jeong, and Y.-L. Park, "Elongatable gripper fingers with integrated stretchable tactile sensors for underactuated grasping and dexterous manipulation," *IEEE Transactions on Robotics*, vol. 38, no. 4, pp. 2179–2193, 2022.

[15] D. Bandara, R. Gopura, G. Kajanthan, M. Brunthavan, and H. Abeynayake, "An under-actuated mechanism for a robotic finger," in *The 4th Annual IEEE International Conference on Cyber Technology in Automation, Control and Intelligent*, pp. 407–412, IEEE, 2014.

[16] R. Abayasiri, R. Abayasiri, R. Gunawardhana, R. Premakumara, S. Mallikarachchi, R. Gopura, T. D. Lalitharatne, and D. Madusanka, "An under-actuated hand prosthesis with finger abduction and adduction for human like grasps," in *2020 6th International Conference on Control, Automation and Robotics (ICCAR)*, pp. 574–580, IEEE, 2020.

[17] Z. Lu, H. Guo, W. Zhang, and H. Yu, "Gtac-gripper: A reconfigurable under-actuated four-fingered robotic gripper with tactile sensing," *IEEE Robotics and Automation Letters*, vol. 7, no. 3, pp. 7232–7239, 2022.

[18] T. Nishimura and T. Watanabe, "Single-motor robotic gripper with three functional modes for grasping in confined spaces," *IEEE Robotics and Automation Letters*, 2023.